NUCKS1 promotes the progression of colorectal cancer via activating PI3K/AKT/mTOR signaling pathway

Liao-Liao ZHU#, Jing-Jie SHI#, Yong-Dong GUO#, Cheng YANG, Rong-Lin WANG, Shan-Shan LI, Dong-Xue GAN, Pei-Xiang MA, Jun-Qiang LI*, Hai-Chuan SU*

Department of Oncology, Tangdu Hospital, Air Force Medical University, Xi'an, Shaanxi, China

Correspondence: jjunqiang@126.com; suhc@fmmu.edu.cn
#Contributed equally to this work.

Nuclear ubiquitous casein and cyclin-dependent kinase substrate 1 (NUCKS1) is highly expressed in a variety of malignant tumors and functions as an oncogene; however, its role in colorectal cancer (CRC) remains unclear. We aimed to explore the function and regulatory mechanisms of NUCKS1 and potential therapeutic agents targeting NUCKS1 in CRC. We knocked down and overexpressed NUCKS1 in CRC cells and explored its effects *in vitro* and *in vivo*. Flow cytometry, CCK-8, Western blotting, colony formation, immunohistochemistry, in vivo tumorigenic, and transmission electron microscopy analyses were performed to determine the effects of NUCKS1 on CRC cell function. LY294002 was used to examine the mechanism of NUCKS1 expression in CRC cells. Potential therapeutic agents for NUCKS1-high CRC patients were analyzed using the CTRP and PRISM datasets, and the function of selected agents was determined by CCK-8 and Western blotting. We revealed that NUCKS1 was highly expressed in CRC tissues and clinically correlated with poor prognosis in CRC patients. NUCKS1 knockdown induces cell cycle arrest, inhibits CRC cell proliferation, and promotes apoptosis and autophagy. These results were reversed when NUCKS1 was overexpressed. Mechanistically, NUCKS1 exerts a cancer-promoting function by activating the PI3K/AKT/mTOR signaling pathway. This was reversed when LY294002 was used to inhibit the PI3K/AKT pathway. Furthermore, we determined that mitoxantrone exhibited high drug sensitivity in NUCKS1-overexpressing CRC cells. This work demonstrated NUCKS1 plays a crucial role in CRC progression via the PI3K/AKT/mTOR signaling pathway. Additionally, mitoxantrone may be a potential therapeutic agent for CRC treatment. Therefore, NUCKS1 represents a promising anti-tumor therapeutic target.

Key words: NUCKS1; proliferation; apoptosis; autophagy; mitoxantrone; colorectal cancer

Colorectal cancer (CRC) is the third most common cancer and accounts for approximately 6.1% of all cases [1]. By 2030, more than 2.2 million new cases and 1.1 million deaths are expected each year [2]. Currently, CRC therapy consists of local surgical resection, chemotherapy based on fluoropyrimidine monotherapy or multiple-drug treatment, immunotherapy, and targeted therapy [3]. However, traditional treatment options are limited, their efficacy is poor, and the clinical application of pioneering immunotherapy also possesses certain limitations. The 5-year survival rate of patients with advanced colorectal cancer is as low as 12.5%, and the prognosis is poor [4]. Therefore, there is an urgent need to identify new specific targets and useful biomarkers to better elucidate the pathogenesis of CRC and use these new targets for clinical treatment.

Nuclear casein kinase and cyclin-dependent kinase substrate 1 (NUCKS1) was discovered more than three decades ago [5] and can be hyperphosphorylated by kinases, cyclin-dependent kinases, and DNA-activated protein kinases [6]. NUCKS1 is highly expressed in various cancers. Studies have demonstrated that NUCKS1 expression is significantly elevated in breast cancer [7, 8] and liver cancer [9]. Additionally, NUCKS1 can affect the cell cycle and cell proliferation. For example, NUCKS1 is recruited to chromatin as a transcription factor and promotes tumor cell entry into the S phase [10]. NUCKS1 is associated with the progression and recurrence of cervical squamous cell carcinoma progression and recurrence [11]. NUCKS1 overexpression promotes xenograft tumor growth [9, 12]. A recent report has demonstrated that NUCKS1 inhibits autophagy and promotes cell proliferation in gastric cancer [13]. Moreover, NUCKS1 enhances the proliferation and invasion of gastric cancer cells [14] and non-small cell lung cancer cells [12]. These findings suggest that NUCKS1 exhibits oncogenic properties, and

NUCKS1 has emerged as a promising biomarker for multiple cancers. However, the ability of NUCKS1 to exert the same effect in CRC and the mechanisms underlying the role of NUCKS1 in the context of CRC remain unknown.

Patients and methods

Patient tissue specimens. We obtained 13 paired CRC and paracancerous tissue samples from Xijing Hospital affiliated with the Air Force Medical University (Xi'an, China). All CRC patient specimens were confirmed by histopathology, and the patients did not receive anti-tumor treatment before surgery. All patients signed an informed consent form to participate in this study. Our study was ethically supported by the ethics committee of the Tangdu Hospital (Medical Ethics Committee approval number: No. 202203-109).

Cell culture. Human colorectal cancer cell lines were purchased from Procell Life Science & Technology Company (Wuhan, China). HCT116 and HT29 cells were maintained in McCoy's 5A medium (HyClone, USA), DLD1 cells were cultured in RPMI-1640 medium (HyClone, USA), and SW480, SW1116, SW620, and LOVO cells were maintained in Dulbecco's modified Eagle's medium (HyClone, USA) supplemented with 10% fetal bovine serum (Gibco, USA) at 37 °C in a humidified incubator with 5% CO_2.

Plasmid transfection and lentiviral infection. The plasmids shNUCKS1#1 and shNUCKS1#2 and the negative control Plko.1-U6-shGFP-puro were purchased from Vigene Biosciences (Jinan, China). The human NUCKS1 gene was used to construct an overexpression plasmid (NUCKS1-OE) in p-CDH-CMV-EGFP-puro (Vigene Biosciences, Jinan, China). shRNA and overexpression plasmid transfections were performed using the HighGene transfection reagent (RM09014, Abclonal, Wuhan, China). Lentiviruses were packaged by co-transfecting HEK293T cells with the expression vector and packaging plasmids (pMD2G and psPAX2) according to the manufacturer's instructions. The shRNA sequences used were as follows: shRNA#1: CCGGGTT-GTTGATTACTCACAGTTTCTCGAGAAACTGTGAG-TAATCAACAACTTTTTG; shRNA#2: CCGGCACTCAG-CAGAGGATAGTGAACTCGAGTTCACTATCCTCTGCT-GAGTGTTTTTG.

We used the viral supernatant to infect cells with the addition of 4 µg/ml polybrene (40804ES76; YEASEN, Shanghai, China). After 12 h, the cells were selected using 6 µg/ml puromycin (13884; Cayman, USA). Finally, stable CRC cells were established.

Western blotting. Lysis of human CRC cell lines or tumor tissues was performed using RIPA buffer (Applygen, Beijing, China) supplemented with a cocktail of protease and phosphatase inhibitors (Roche, Branchburg, USA). SDS-PAGE (Beyotime, Shanghai, China) was used to separate the proteins that were then transferred onto PVDF membranes (IPVH00010, Millipore, USA). The PVDF membranes were blocked with 5% non-fat milk for 2 h. The sections were then incubated with primary antibodies at 4 °C overnight and with secondary antibodies for 1 h at room temperature. Finally, the protein bands were visualized using an ECL Western Blot Kit (Zhuangzhibio, Xi'an, China).

The primary antibodies that included anti-NUCKS1 (12023-2-AP), anti-GAPDH (60004-1-Ig), anti-P62/SQSTM1 (18420-1-AP), anti-CyclinA2 (66391-1-Ig), anti-CyclinD1 (26939-1-AP), and anti-Bcl2 (12789-1-AP) were purchased from Proteintech of USA, anti-Cleaved PARP (Asp214) (#5625), anti-PARP (#9532), and anti-p-H$_2$AX(Ser139) (#9718), anti-AKT (#4691), anti-p-AKT (Ser-473) (#4060), anti-phospho-mTOR (Ser2448) (#5536) were purchased from Cell Signaling Technology of USA, anti-mTOR (A11355), anti-LC3B (A19665), and anti-phospho-EIF4EBP1 (Thr37/46) (AP0030), anti-4EBP1 (A19045) were acquired from ABclonal of China. The secondary antibodies that included HRP goat anti-rabbit IgG (AS014) and HRP goat anti-mouse IgG (AS003) were from ABclonal (China). In the detection of autophagy protein LC3B, autophagy inhibitors Chloroquine (CQ, 20 µM; MCE, USA) and Aloxistatin (E64d, 10 µg/ml; Abcam, Cambridge, UK) were used.

Quantitative real-time PCR (q-PCR). Total RNA was extracted from the cells following the instructions of the M5 Universal RNA Mini Kit (Mei5Bio, Beijing, China). We used the HiScript II Q RT SuperMix kit (Vazyme, Nanjing, China) to reverse transcribe RNA into cDNA, and ChamQ SYBR Qpcr Master Mix (Vazyme) was used to perform real-time PCR. The primers used for this study included:

NUCKS1 (forward: 5'-GGGCAGTGAGGAAGAACAA-3', reverse: 5'-TTGATGCCTTTGAAGCTGTG-3') and GAPDH (forward: 5'-GGAGTCCACTGGCGTCTTCA-3', reverse: 5'-GTCATGAGTCCTTCCACGATACC-3').

Cell counting kit 8 (CCK-8). First, cells were seeded in 96-well plates. For cell proliferation assays, 10 µL of CCK-8 (7sea biotech, Shanghai, China) was added to each well at 6, 24, 48, and 72 h. For cytotoxicity assays, cells were cultured for 24 h, different concentrations of mitoxantrone (MCE, USA) were added at 24, 48, and 72 h, then 10 µl CCK-8 was added into each well. After 2 h of incubation in the cell culture incubator, the absorbance was detected at 450 nm. Three independent experiments were conducted. Cell viability rate = [(experimental well blank well)/(control well blank well)] × 100%.

Colony formation assay. The collected cells were seeded at a density of 1,000 cells/well into 6-well plates. The PI3K/AKT pathway inhibitor LY294002 (Cell Signaling Technology, USA) was added to the cells at a concentration of 10 µM. After 12 days, the cells were fixed using methanol (Tianli, Tianjin, China) for 5 min and stained with 1% crystal violet (ZHHC, Shanxi, China) for 30 min. Finally, the cells were washed with running water to visualize colony formation ability. Three independent experiments were conducted.

Immunohistochemistry (IHC). The patient tissue specimens and nude mouse subcutaneous tumor tissues were fixed in 4% paraformaldehyde (Servicebio, Wuhan, China) for 24 h

and then embedded in paraffin. Experiments were performed according to the instructions of the rabbit SP kit (SP-9001; ZSGB-BIO, Beijing, China), and staining with anti-NUCKS1 (1:100, 12023-2-AP; Proteintech, USA), anti-Ki67 (2 µg/ml, ab15581; Abcam, USA), anti-p-AKT (Ser-473) (1:50, #4060; Cell Signaling Technology, USA), and anti-phospho-mTOR (Ser2448) (1:50, #5536; Cell Signaling Technology, USA) was performed. Sodium citrate antigen retrieval solution (50×) (Solarbio, Beijing, China) and hematoxylin (Sbjbio, Nanjing, China) were used. The sections were then washed with 1× PBS (Servicebio, Wuhan, China). ImageJ software was used to count the positive signals.

Flow cytometry assay. For cell cycle distribution analysis, cells were cultured in 6-well plates for 24 h, collected, and then resuspended in cold 75% alcohol overnight at 4°C. Cells were washed twice with 1× PBS and incubated with PI/RNase staining buffer (BD Biosciences, USA) for 15 min. Finally, the stained cells were detected using flow cytometry (Thermo Fisher Scientific, USA) with cell cycle detection (BD FACSCalibur, USA). The data were analyzed using ModFitLT software.

For apoptosis analysis, cells were cultured in 6-well plates for 48 h, and the cells and supernatants were collected, centrifuged, and washed twice with 1× PBS. The Annexin V-Alexa Fluor 647/7-AAD Kit (4A Biotech, Beijing, China) was used to stain the cells. We resuspended $1×10^5$ cells in 100 µl of 1× binding buffer, added 5 µl of Annexin V/Alexa Fluor 647 and 10 µl of 7-AAD, and incubated the cells for 5 min in the dark. Finally, 400 µl of 1× binding buffer was added to the stained cells that were then detected using flow cytometry (BD FACSCalibur, USA). The maximum emission wavelengths of Annexin V-Alexa Fluor 647 and 7-AAD are 668 nm and 647 nm, respectively, which are detected in the FL4 and FL3 channels of flow cytometry. The results were analyzed using FlowJo_V10. Three independent experiments were conducted.

***In vivo* tumorigenic assay.** Female BALB/c nude mice (6–8 weeks old, 18–22 g) were purchased from the Experimental Animal Centre of Air Force Medical University (Xi'an, China) and maintained in an SPF environment. Each mouse was injected subcutaneously with colorectal cancer cells ($3×10^6$ HCT116 cells) to establish a CRC subcutaneous transplantation tumor model. Tumor volume was measured every three days using calipers (volume = length × width^2 × 0.5). After three weeks, the mice were euthanized, and the tumor tissues were collected and weighed. Finally, the tumor tissues were fixed and preserved in 4% paraformaldehyde. All experimental procedures were approved by the Institutional Animal Care and Use Committee of Tangdu Hospital. (Number: 20220730).

Potential therapeutic agents for high NUCKS1 CRC patients. We used two approaches, Cancer Therapeutics Response Portal (CTRP, https://portals.broadinstitute.org/ctrp) and PRISM Repurposing dataset (https://depmap.org/portal/prism/) to identify candidate agents for CRC patients

with high NUCKS1. Then we performed Spearman rank correlation analysis between NUCKS1 and AUC value to identify agents with negative correlation coefficient (R<−0.20 for CTRP and PRISM, p<0.05). We screened five agents via CTRP and nine agents via the PRISM dataset. The lower the AUC value as a measure of drug sensitivity, the higher the drug sensitivity to treatment. Differential agents sensitivity between NUCKS1-low (bottom decile) and NUCKS1-high (top decile) was analyzed via the Wilcox rank sum test to identify agents with lower estimated AUC values in the former (log2FC>0.1).

Statistical analysis. The data are expressed as "mean ± SD" and were analyzed using GraphPad Prism 8.0 and SPSS Statistics 25.0. The differences between two groups were analyzed using Student's t-test, and one-way ANOVA was used for comparisons among three or more groups. Pearson correlation analysis was used to assess the association between NUCKS1 and Ki-67 positive areas in CRC tissue specimens. Statistical tests were two-tailed, and a p-value <0.05 was considered statistically significant.

Results

NUCKS1 expression is upregulated in CRC and is significantly correlated with poor patient prognosis. The gene expression of NUCKS1 in different human cancer tissues was analyzed using the ONCOMINE database, and the results indicated that NUCKS1 mRNA levels were significantly higher in eleven cancer tissues comprising colorectal cancer (CRC) compared to levels in the corresponding normal tissues (Figure 1A). TCGA RNA-seq data from TIMER revealed that NUCKS1 mRNA expression was remarkably higher in multiple tumors, including colon adenocarcinoma (COAD) (Figure 1B). The expression of NUCKS1 in CRC was further assessed using TCGA data, and it was observed that NUCKS1 was remarkably overexpressed in CRC tissues compared to levels in normal tissues (Figures 1C, 1D). IHC staining of CRC patient tissue specimens confirmed that NUCKS1 was upregulated in tumor tissues and downregulated in normal tissues (Figure 1E). We also evaluated NUCKS1 protein levels in tissues from 13 CRC patients by western blotting and observed that the ratio of patients with high expression of NUCKS1 in tumor tissues to those with high expression of NUCKS1 in normal tissues was 9/4, and this further indicated that NUCKS1 was highly expressed in CRC tumor tissues (Figure 1F). The human CRC cell lines HT29, HCT116, LOVO, and SW620 expressed NUCKS1 at higher levels than did DLD1, SW480, and SW1116 cells at the protein level (Figure 1G). Moreover, these cells exhibited a relatively high expression of NUCKS1 at the RNA level (Figure 1H). The expression distribution of NUCKS1 mRNA in different cell lines obtained from the CCLE dataset [15] also revealed that NUCKS1 was highly expressed in different CRC cell lines (Figure 1I). Differential expression of NUCKS1 with different clinical characteris-
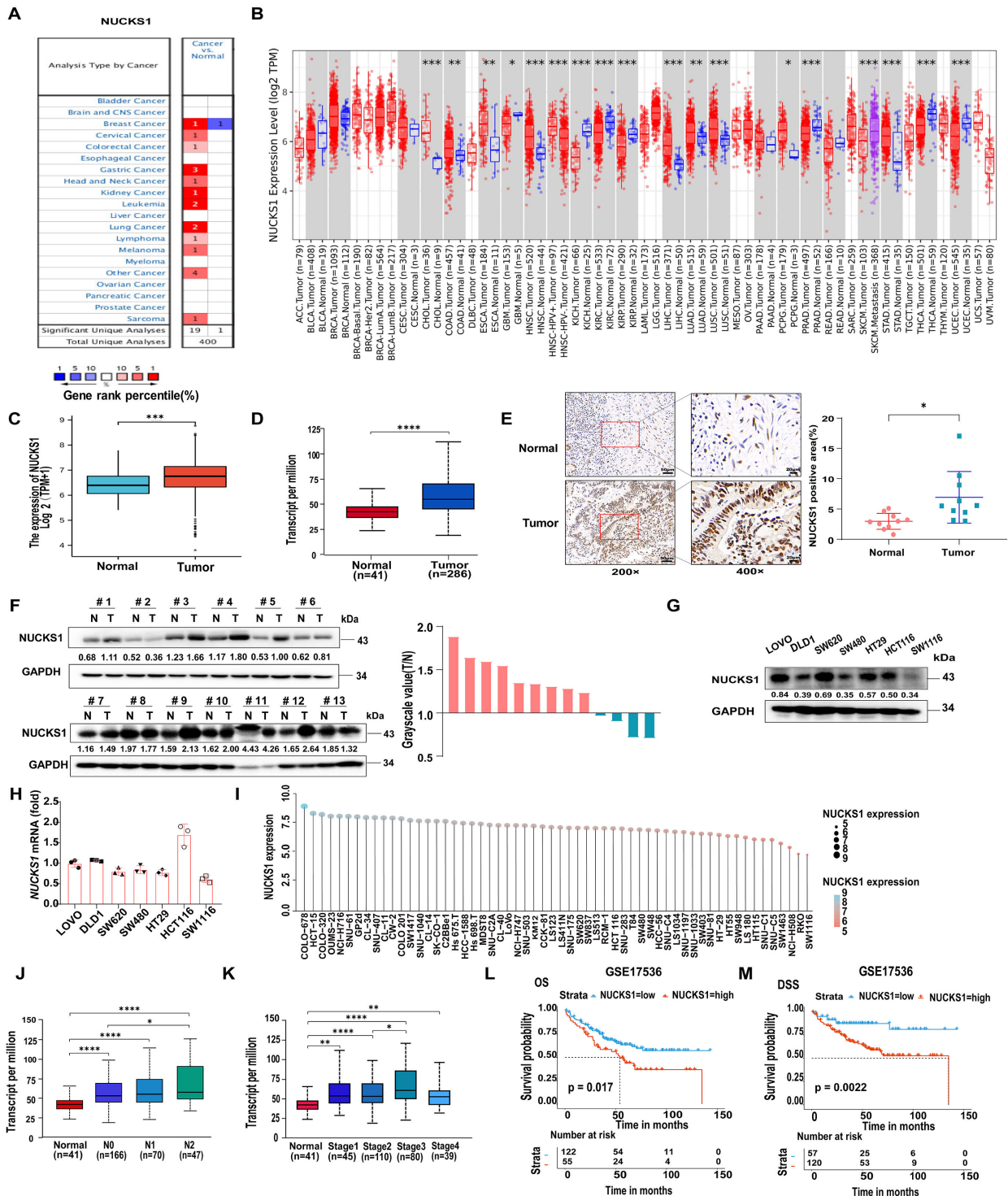
Figure 1. NUCKS1 was overexpressed in CRC, and NUCKS1 expression was associated with poor prognosis in CRC patients. A) The expression of NUCKS1 in various human cancer tissues from the Oncomine database. **B)** The expression levels of NUCKS1 in different tumor types. **C)** The NUCKS1 mRNA expression from TCGA RNA-seq data using Xiantao Academic. **D)** The expression of NUCKS1 in normal tissues and CRC tissues using UALCAN. **E)** The IHC staining of NUCKS1 in normal and tumor tissues. **F)** The protein levels of NUCKS1 in tissues from 13 CRC patients. The numbers under the bands indicate relative protein expression levels. **G)** The levels of NUCKS1 in CRC cell lines. **H)** The mRNA level of NUCKS1 in CRC cell lines. **I)** The NUCKS1 mRNA expression in different CRC cell lines from the CCLE dataset. **J)** The correlation of NUCKS1 expression with nodal metastasis status from TCGA in UALCAN. **K)** The correlation of NUCKS1 expression with individual cancer stages from TCGA in UALCAN. **L–M)** Kaplan-Meier analysis of the association between NUCKS1 expression and OS (Overall Survival) (L), or DSS (Disease Free Survival) (M) in CRC. *p<0.05, **p<0.01, ***p<0.001, ****p<0.0001

tics detected by UALCAN indicated that NUCKS1 expression was markedly correlated with nodal metastasis status (Figure 1J) and individual cancer stages (Figure 1K). Subsequently, we analyzed the prognostic assessment value of NUCKS1 expression in GSE17536 from TCGA using the Cox proportional hazards model and Kaplan-Meier analysis, the results confirmed that high NUCKS1 expression was associated with poorer OS (p=0.017) and shorter DSS (p=0.0022) in the context of CRC (Figures 1L, 1M). Collectively, these results suggest that NUCKS1 is highly expressed in CRC and is associated with poor prognosis in patients with CRC.

NUCKS1 promotes CRC cell proliferation *in vitro* and *in vivo*. To determine the effects of NUCKS1 on CRC cell proliferation, we first analyzed gene enrichment pathways using NUCKS1 ChIP-Seq data [16]. In the top 20 identified gene ontology biological process (GO BP) clusters, NUCKS1 and regulation of the mitotic cell cycle were highly interrelated (Figure 2A). We then stably silenced NUCKS1 in wild-type human CRC cells (HCT116 and HT29) using short hairpin-mediated RNA interference (shNUCKS1), and western blotting (Figure 2B) and q-PCR (Figure 2C) detection indicated that intracellular NUCKS1 levels were significantly reduced. Meanwhile, we generated SW480 and DLD1 cells overexpressing NUCKS1 (NUCKS1-OE). NUCKS1 expression was detected by western blotting (Figure 2D) and q-PCR (Figure 2E), both of which indicated that NUCKS1 was successfully overexpressed compared to levels in the control (NC). Subsequently, we tested the effect of NUCKS1 on the cell cycle, and flow cytometry analysis revealed that NUCKS1 functions during the G1/S transition. NUCKS1 knockdown in HCT116 and HT29 arrested cells in the G1 phase and inhibited S phase entry (Figures 2F–2G). NUCKS1 overexpression in SW480 and DLD1 cells promoted the transition from G1 to S phase (Figures 2H, 2I). To elucidate the mechanism by which NUCKS1 affects the cell cycle, we examined the protein levels of CyclinD1 and CyclinA2 which are essential cell cycle regulators and play key roles in cell cycle progression [17]. As expected, the levels of cyclin D1 and cyclin A2 were decreased in NUCKS1-silenced HCT116 and HT29 cells (Figure 2J). The levels of two proteins were notably increased in the cells overexpressing NUCKS1 (Figure 2K).
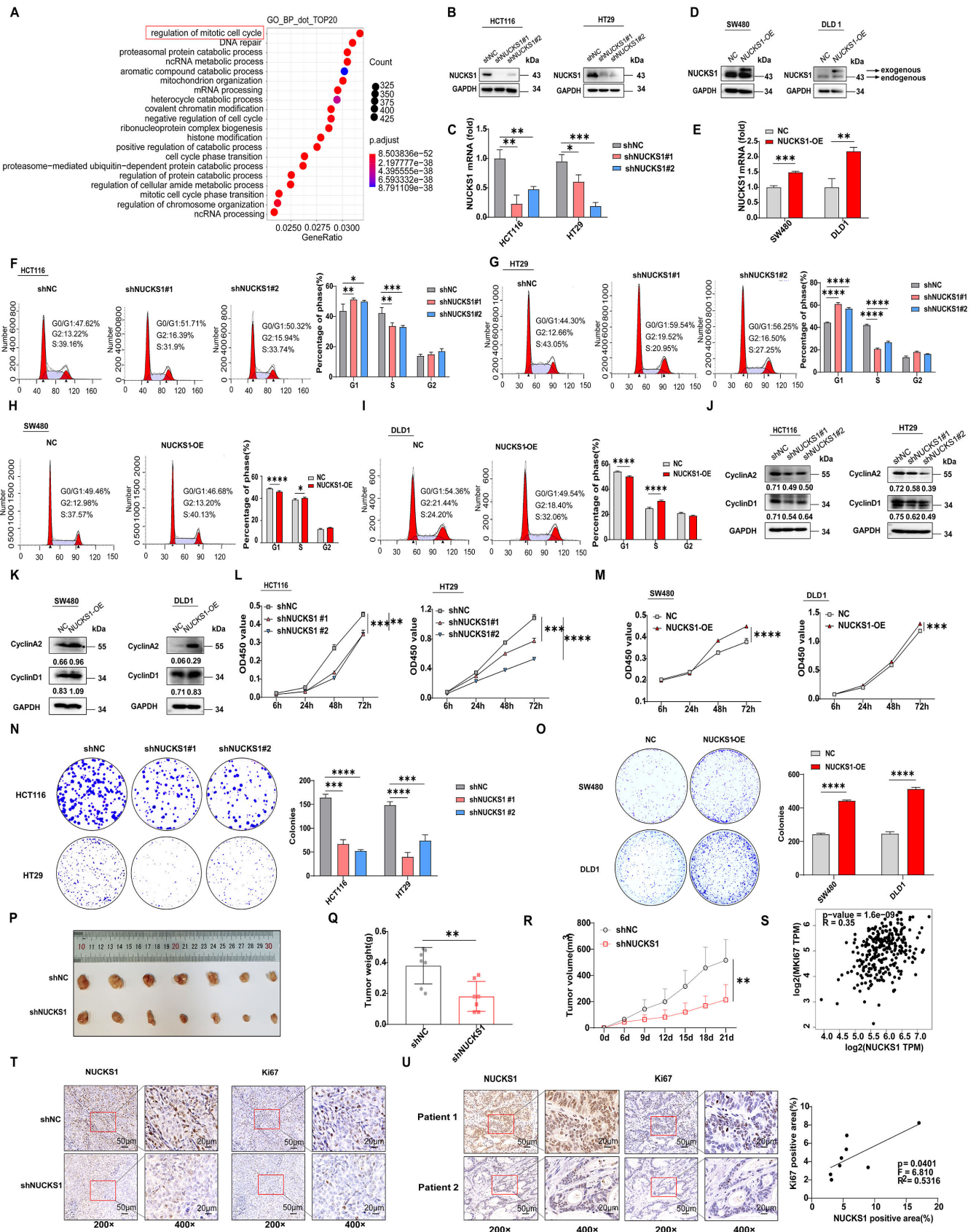
Moreover, CCK-8 assay results indicated that NUCKS1 knockdown inhibited the proliferative activity of HCT116

and HT29 cells (Figure 2L). And overexpression of NUCKS1 significantly promoted cell proliferation over a 72 h culture period (Figure 2M). Consistent with the proliferation data, the knockdown of NUCKS1 significantly reduced the colony-forming ability of both cell lines (Figure 2N). The NUCKS1 overexpression increased the colony formation ability of cells (Figure 2O).

HCT116 cells were subcutaneously injected into BALB/c nude mice to study the role of NUCKS1 *in vivo*. Tumor weight was lower in the NUCKS1 silencing group than it was in the negative control group (shNC), and NUCKS1 knockdown suppressed tumor growth (Figures 2P, 2R). The correlation between NUCKS1 and Ki-67 was further analyzed using TCGA database in GEPIA, and NUCKS1 and Ki-67 were significantly positively correlated (Figure 2S). Furthermore, we detected NUCKS1 and Ki-67 expression in mouse tumor tissues. IHC staining of tumor tissues for NUCKS1 and Ki-67 indicated that Ki-67 was downregulated in the NUCKS1-silenced group (Figure 2T). Among the collected specimens from CRC patients, eight specimens were randomly selected for serial sectioning, and the results of IHC staining indicated that when NUCKS1 was highly expressed, Ki-67 was also highly expressed in the patient specimens. Additionally, the proportion of positive areas of NUCKS1 and Ki-67 were positively correlated (Figure 2U). Collectively, our findings suggest that NUCKS1 promotes cell cycle progression and CRC cell proliferation, and NUCKS1 knockdown reduces CRC cell tumorigenesis.

NUCKS1 suppresses apoptosis of CRC cells. Numerous physiological processes require co-regulation of proliferation and apoptosis [18]. Apoptosis exerts an important impact on the occurrence, development, and drug resistance of tumors [19]. Thus, to further examine the role of NUCKS1 in CRC cells, flow cytometry was used to analyze the role of NUCKS1 in cell apoptosis. We determined that the knockdown of NUCKS1 enhanced apoptosis in HCT116 and HT29 cells (Figures 3A, 3B). Additionally, we observed that NUCKS1-overexpressing SW480 and DLD1 cells exhibited significantly reduced apoptosis compared to that of the NC group (Figures 3C, 3D). We then tested the expression of apoptosis-related proteins using western blotting. As observed, in HCT116 and HT29 cells knockdown of NUCKS1 markedly promoted the conversion of PARP to cleaved PARP, the

Figure 2. NUCKS1 promoted CRC cell proliferation and tumor growth. A) The GO enrichment analysis of NUCKS1 ChIP-Seq data (accession code GSE58100). **B)** The NUCKS1 expression was measured using western blotting in two constructed stable CRC cells. **C)** The mRNA levels of NUCKS1 in two cells were measured using q-PCR. **D)** The protein levels of NUCKS1 in the constructed stable cells SW480 and DLD1. **E)** The mRNA levels of NUCKS1 in two CRC cells. **F–I)** Representative images (left) and quantification of cell cycle distribution (right). **J–K)** The levels of CyclinD1 and CyclinA2 were detected by western blotting. The numbers under the bands indicate relative protein expression levels. **L)** CCK-8 assays for HCT116 and HT29 cells expressing shNUCKS1#1, shNUCKS1#2, or shNC. **M)** CCK-8 assays in stable NUCKS1-overexpressing SW480 and DLD1 cells. **N)** Colony formation assays for shNUCKS1 and shNC cells. **O)** Colony formation assays in NUCKS1 overexpression and NC cells. **P)** Representative images of tumors formed subcutaneously in nude mice with 7 mice per group. **Q)** The tumor weights were measured after the observation experiments. **R)** Tumor volumes were measured every three days after tumors were observed on day six, and tumor growth curves were plotted. **S)** The correlation of NUCKS1 and Ki67 in CRC from TCGA data in GEPIA. **T)** Expression of NUCKS1 and Ki-67 in mice tumor tissue sections was determined by IHC. **U)** The tissue samples of CRC patients were stained with NUCKS1 and Ki-67. Typical IHC images stained with NUCKS1 and Ki-67 were presented (left), and correlation analysis of these two proteins was presented (right). Magnification: ×200 and ×400, scale bars 50 μm and 20 μm, respectively. *p<0.05, **p<0.01, ***p<0.001, ****p<0.0001

A

GO_BP_dot_TOP20

regulation of mitotic cell cycle
DNA repair
proteasomal protein catabolic process
ncRNA metabolic process
aromatic compound catabolic process
mitochondrion organization
mRNA processing
heterocycle catabolic process
covalent chromatin modification
negative regulation of cell cycle
ribonucleoprotein complex biogenesis
histone modification
positive regulation of catabolic process
cell cycle phase transition
proteasome−mediated ubiquitin−dependent protein catabolic process
regulation of protein catabolic process
regulation of cellular amide metabolic process
mitotic cell cycle phase transition
regulation of chromosome organization
ncRNA processing

Count
325
350
375
400
425

p.adjust
8.503836e-52
2.197777e-38
4.395555e-38
6.593332e-38
8.791109e-38

anti-apoptotic protein Bcl-2 was decreased, and the p-H$_2$AX that is crucial in the response to DNA damage [20] was remarkably increased in shNUCKS1#1 and shNUCKS1#2 cells (Figures 3E, 3F). Consistent with the above results, we observed that in NUCKS1-overexpressing SW480 and DLD1 cells, the protein levels of cleaved PARP and p-H$_2$AX were lower than were those in the NC group and that Bcl-2 was higher than that in the NC group (Figures 3G, 3H). These results suggest that NUCKS1 inhibits apoptosis in CRC cells.

NUCKS1 inhibits CRC autophagy activation. Similar to apoptosis, autophagy represents an important cellular physiological response in the context of cancer [21–23]. KEGG enrichment analysis of the NUCKS1 ChIP-Seq data demonstrated that the related genes were markedly enriched in colorectal cancer pathways and were highly correlated with autophagy (Figure 4A). As the lipidated form (LC3BII) of LC3B correlates with autophagosome abundance and P62 is a marker of autophagy inhibition [24, 25], we estimated the levels of LC3BII and P62. Increased LC3BII and decreased p62 expression were detected in NUCKS1-silenced HCT116 and HT29 cells (Figure 4B) while NUCKS1-overexpressing SW480 and DLD1 cells exhibited lower LC3BII and higher P62 levels compared to levels in the NC group (Figure 4C). To further understand the regulation of autophagy by NUCKS1, we analyzed the regulation of autophagy by NUCKS1 in CRC cells treated with autophagy inhibitors such as chloroquine (CQ) and E64d. CQ has been reported to interrupt autophagy by inhibiting the acidification of the lysosome [26]. We tested the levels of LC3BII with or without CQ in NUCKS1-silenced HCT116 and HT29 cells and also in NUCKS1-overexpressing SW480 and DLD1 cells. We observed that the expression of LC3BII was increased in CRC cells treated with CQ for 8 h compared to levels in cells without CQ, while in CQ-treated cells, the expression of LC3BII remained higher in the shNUCKS1 group than it was in the shNC group (Figures 4D, 4E). Correspondingly, in CQ-treated cells, the expression of LC3BII was lower in the NUCKS1 overexpression group than it was in the NC group (Figures 4F, 4G). In addition, we found that the ratio of LC3BII/LC3BI (the higher the ratio, the higher the autophagy level) in the NC group in Figure 4C was lower than that in the NC group without CQ treatment in Figure 4F and Figure 4G. The occurrence of autophagy is a dynamic process [27]. Therefore, we believed that this may be caused by the different time of collecting SW480 and DLD1 cells. The cells in Figure 4C were collected and extracted proteins after 24 h of culture, while the cells in Figure 4F and 4G continued to be cultured for 8 h after 24 h of culture. Moreover, CRC cells were treated with E64d, another agent that inhibits autophagy by inhibiting lysosomes [28], and the results revealed that CRC cells treated with E64d for 24h expressed higher levels of LC3BII than did cells without E64d. In CRC cells treated with E64d, the expression of LC3BII was considerably increased in the NUCKS1 knockdown group, and LC3BII was notably reduced in the

NUCKS1 overexpression group (Figures 4H–4K). Additionally, NUCKS1-silenced HCT116 and HT29 cells displayed more autophagosomes with double-membrane vacuoles than did shNC cells (Figures 4L, 4M, 4P, 4Q). However, NUCKS1-overexpressing SW480 and DLD1 cells exhibited fewer autophagosomes than did the NC group (Figures 4N, 4O, 4R, 4S). These results indicated that NUCKS1 reduces autophagosome accumulation in CRC cells.

NUCKS1 promotes CRC progression by activating the PI3K/AKT/mTOR signaling pathway. Based on the above effects of NUCKS1 on the CRC cell phenotype, we further explored the molecular mechanism by which NUCKS1 regulates CRC cells. The PI3K/AKT/mTOR signaling pathway is activated in most human cancers [29]. This pathway regulates tumor cell proliferation, growth, survival, and angiogenesis and plays a crucial role in colorectal carcinogenesis [30]. Therefore, western blotting was used to detect the key molecules of the PI3K/AKT/mTOR signaling pathway. We determined that the ratios of p-AKT/AKT, p-mTOR/mTOR, and p-4EBP1/4EBP1 were significantly reduced in NUCKS1-silenced HCT116 and HT29 cells compared to those in shNC cells (Figures 5A, 5B). The protein 4EBP1 is a downstream mediator of mTOR and is an important factor in the synthesis of certain oncogenic proteins [31]. Simultaneously, we observed that the ratios of the same proteins were markedly upregulated in NUCKS1-overexpressing SW480 and DLD1 cells (Figures 5C, 5D). Furthermore, IHC staining of nude mice tumor tissues for p-AKT and p-mTOR in the shNC and NUCKS1-silenced groups revealed reduced levels of p-AKT and p-mTOR in the shNUCKS1 group (Figure 5E). These data indicate that NUCKS1 functions through the PI3K/AKT/mTOR signaling pathway. To further confirm this, we treated NUCKS1-overexpressing SW480 and DLD1 cells with LY294002, a typical PI3K/AKT pathway inhibitor that decreases the expression levels of p-AKT [32]. After treatment with LY294002, the ratio of p-AKT/AKT was decreased compared to that in the NUCKS1-overexpressing group (Figures 5F–5H).

Next, colony formation assay and CCK-8 assay were performed to examine the proliferation of CRC cells when p-AKT levels were downregulated by LY294002. The results indicated that NUCKS1 overexpression promoted the ability to form colony formation and increased cell proliferation; however, when p-AKT was reduced by LY294002, cell proliferation was inhibited (Figures 5I–5M). Concurrently, apoptosis was considerably increased in LY294002-treated NUCKS1-overexpressing SW480 and DLD1 cells compared to that in untreated cells (Figures 5N, 5O). Additionally, increased LC3BII and reduced P62 levels were observed in LY294002-treated cells compared to levels in untreated cells, thus suggesting increased autophagy when p-AKT was decreased (Figures 5P, 5Q). These results indicate that NUCKS1 promotes CRC proliferation and inhibits apoptosis and autophagy by activating the PI3K/AKT/mTOR signaling pathway.
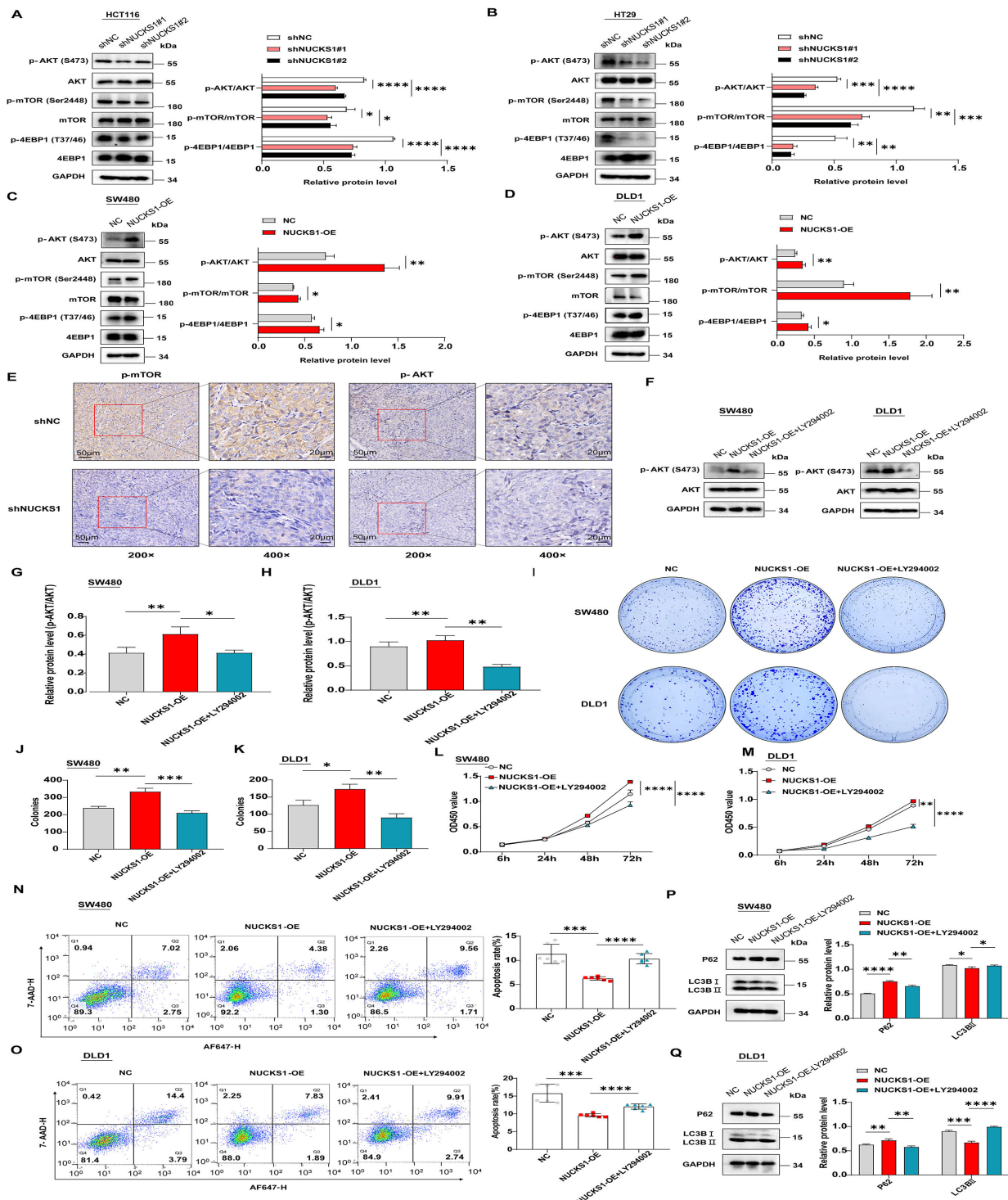
Mitoxantrone is a potential therapeutic agent for CRC patients with high NUCKS1 expression. Based on our conclusion that NUCKS1 promotes CRC progression, we evaluated and identified potential therapeutic agents that are sensitive to NUCKS1. Referring to the methods presented in existing studies [33], the identification of agents with higher
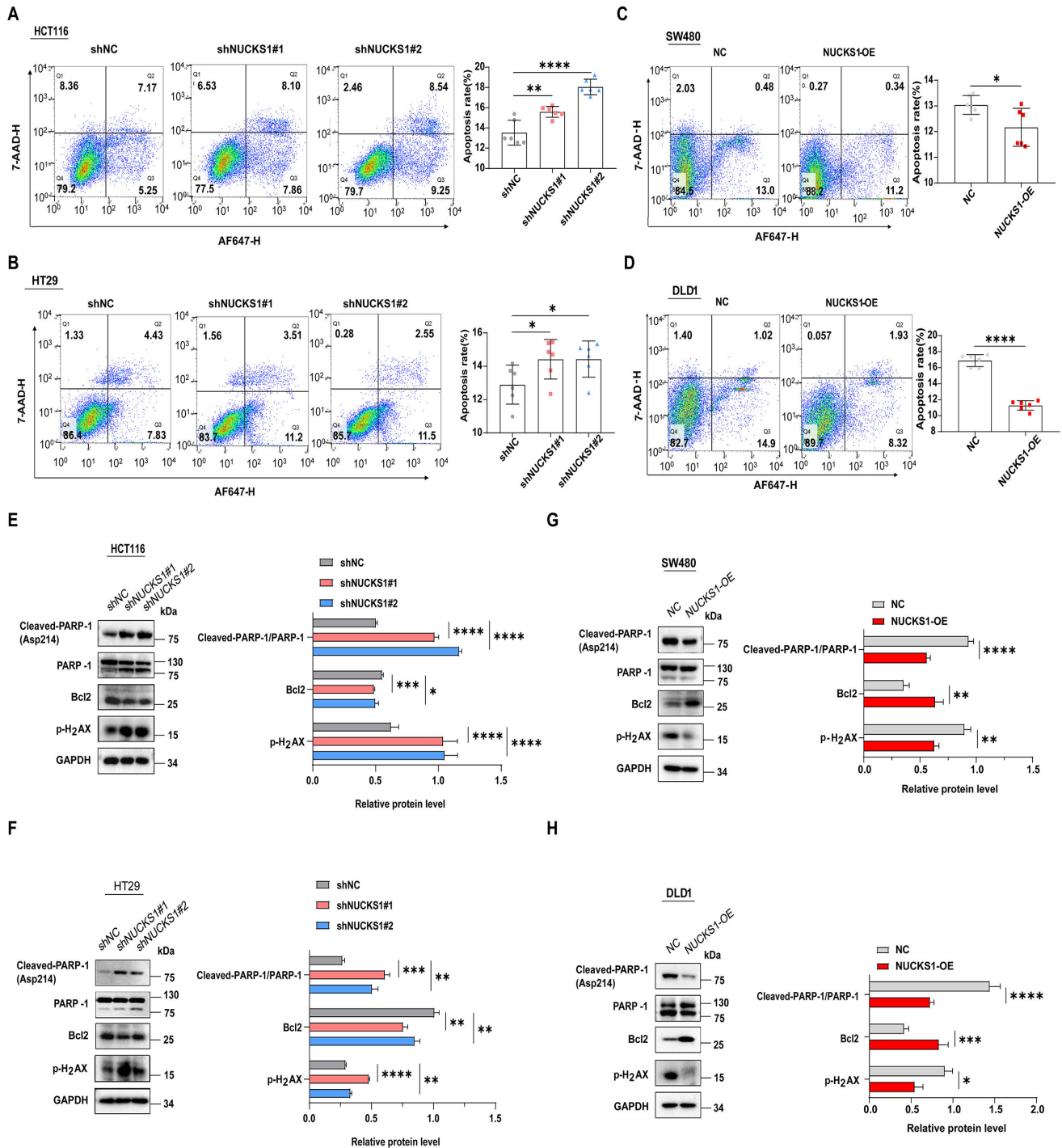
Figure 3. NUCKS1 inhibited cell apoptosis. A, B) HCT116 and HT29 cells were collected after 48h, and apoptosis was detected by flow cytometry. **C, D)** Apoptosis of SW480 and DLD1 cells was detected using flow cytometry. **E, F)** The levels of cleaved PARP, Bcl-2, and p-H2AX were detected using western blotting in shNC and NUCKS1-silenced HCT116 and HT29 cells. **G, H)** Apoptosis-related proteins were also assessed in NC and NUCKS1-overexpressing SW480 and DLD1 cells. *p<0.05, **p<0.01, ***p<0.001, ****p<0.0001

Figure 4. NUCKS1 inhibited the autophagy pathway in CRC cells. A) The KEGG enrichment analysis of NUCKS1 ChIP-Seq data (accession code GSE58100). **B)** The protein levels of LC3BII and P62 in NUCKS1-silenced HCT116 and HT29 cells. The numbers under the bands indicate relative protein expression levels. **C)** Western blotting detected the expression of LC3BII and P62 in SW480 and DLD1 cells overexpressing NUCKS1. **D–E)** Western blotting was used to examine the expression of LC3BII in NUCKS1-silenced HCT116 and HT29 cells that were treated with chloroquine (20 μM) for 8 h. **F, G)** The protein levels of LC3BII were examined in NUCKS1-overexpressing SW480 and DLD1 cells treated with chloroquine (20 μM) for 8 h or in cells that were not treated with chloroquine. **H, I)** The protein levels of LC3BII were detected in NUCKS1-silenced HCT116 and HT29 cells treated with E64d (10 μg/ml) for 24 h. **J, K)** Western blotting detected the levels of LC3BII in NUCKS1-overexpressing SW480 and DLD1 cells treated with E64d (10 μg/ml) for 24 h. **L, M)** Transmission electron microscopy was used to indicate the numbers of autophagosomes in NUCKS1-silenced HCT116 and HT29 cells. **N, O)** Autophagosomes were observed by transmission electron microscopy in NUCKS1-overexpressing SW480 and DLD1 cells. The structure indicated by the red arrow is the autophagosome. Scale bar = 1 μm. **P, Q)** Statistical analysis was performed to calculate the number of autophagosomes in NUCKS1-silenced HCT116 and HT29 cells as indicated by transmission electron microscopy. **R, S)** The number of autophagosomes was calculated in NUCKS1-overexpressing SW480 and DLD1 cells as indicated by transmission electron microscopy. *p<0.05, **p<0.01, ***p<0.001

Figure 5. NUCKS1 promoted CRC progression by regulating the PI3K/AKT/mTOR signaling pathway. A, B) Western blotting was used to detect the levels of critical proteins in the PI3K/AKT/mTOR signaling pathway after NUCKS1 knockdown (left). The ratio of relative protein level (right). **C, D)** The expression of relevant proteins in the PI3K/AKT/mTOR signaling pathway after NUCKS1 overexpression (left). The ratio of relative protein level (right). **E)** The nude mice tumor tissues were stained with p-AKT and p-mTOR. Magnification: ×200 and ×400, scale bars 50 μm and 20 μm, respectively. **F–H)** The levels of p-AKT in NUCKS1-overexpressing SW480 and DLD1 cells treated with LY294002 (10 μM) or in untreated cells (F). Quantification of the results in F (G–H). **I–K)** Cell proliferation was assessed by colony formation assay. Representative images (I), and quantification of the images (J–K). **L, M)** Cell growth ability was detected by CCK-8 assay. **N, O)** Flow cytometric analysis of apoptosis in NUCKS1-overexpressing SW480 and DLD1 cells after treatment of LY294002 (10 μM) for 1 h. Representative images (left) and quantitative analysis (right). **P, Q)** The expression levels of P62 and LC3BII were assessed by western blotting. Quantitative analysis of relative protein level (right). *$p < 0.05$, **$p < 0.01$, ***$p < 0.001$, ****$p < 0.0001$

sensitivity in CRC patients with high NUCKS1 expression was performed using two different approaches (Figure 6A). We used CTRP- and PRISM-derived drug response data. Spearman's correlation analysis between NUCKS1 expression and AUC value was used to select agents with a negative correlation coefficient (Spearman's R<−0.20). Five CTRP-derived and nine PRISM-derived compounds were identified. The estimated AUC values for the identified compounds were analyzed in the NUCKS1-high and NUCKS1-low groups, and we observed that the compounds in the NUCKS1-high group exhibited a lower estimated AUC value, thus implying higher drug sensitivity (Figures 6B, 6C).

Furthermore, among these compounds, mitoxantrone was selected to examine its therapeutic effect in the context of CRC. Mitoxantrone has been used clinically as an anticancer drug for different types of cancer such as breast cancer, prostate cancer, leukemia, and lymphoma [34, 35]. First, we analyzed the relative viabilities of CRC cell lines under different concentrations of mitoxantrone at 24h, 48h, and 72h by CCK-8 assay, and we determined that the cell relative viability gradually decreased with longer treatment time and higher concentrations of mitoxantrone (Figures 6D–6G). Based on these results, we chose mitoxantrone concentrations of 4 μM and 8 μM, and the treatment time was established as 48h to examine the effect of mitoxantrone on NUCKS1 knockdown and overexpression in cells. The CCK-8 assay was used to detect the relative viability of NUCKS1-silenced HCT116 and HT29 cells treated with mitoxantrone, and the results after normalized calculations indicated that NUCKS1 knockdown cells exhibited higher relative viability after mitoxantrone treatment than did shNC cells (Figures 6H, 6I). However, NUCKS1-overexpressing SW480 and DLD1 cells exhibited lower relative viability after mitoxantrone treatment than did NC cells (Figures 6J, 6K). Moreover, Western blotting demonstrated that mitoxantrone induced the cleavage of PARP that was reduced in NUCKS1 knockdown HCT116 and HT29 (Figures 6L, 6M), and the ratio was remarkably upregulated in NUCKS1-overexpressing SW480 and DLD1 cells compared to levels in the NC (Figures 6N, 6O). Taken together, these data suggest that CRC patients with high NUCKS1 levels exhibit a higher drug sensitivity to mitoxantrone that represents a potential future clinical therapy.

Collectively, our study demonstrates that NUCKS1 promotes CRC cell proliferation, inhibits cell apoptosis, and suppresses autophagy by activating the PI3K/AKT/mTOR signaling pathway. Mitoxantrone is a potential therapeutic agent for CRC patients exhibiting high NUCKS1 expression (Figure 6P).

Discussion

NUCKS1 acts as a tumor-promoting factor in different cancers, however, its role in the context of CRC remains unclear. Our study revealed that NUCKS1 is a crucial regulator of CRC progression. From *in vivo* studies, we determined that NUCKS1 knockdown in CRC cells inhibited their subcutaneous tumor growth in nude mice, and this is consistent with previous research findings [9, 11]. *In vitro* studies have also demonstrated that NUCKS1 overexpression in CRC cells promotes proliferation and suppresses apoptosis.

A previous study has indicated that NUCKS1 is a key molecule in the checkpoint pathway for the G1/S transition [10]. Therefore, western blotting and flow cytometry were used to investigate cell cycle progression. We observed that NUCKS1 overexpression enhanced the protein levels of CyclinA2 and CyclinD1 and promoted the G1/S transition. Uncontrolled cell proliferation caused by cell cycle dysregulation is a hallmark of cancer [36]. We further detected cell proliferation using CCK-8 and colony formation assays, and the results revealed that NUCKS1 overexpression promoted CRC cell proliferation.

Apoptosis and proliferation are intimately coupled [37]. Previous studies have demonstrated that Bcl2 is a key protein regulating cell apoptosis. High expression of Bcl2 can inhibit cell apoptosis, accelerate cell growth, and lead to the occurrence of malignant tumors [38, 39]. p-H$_2$AX plays a key role in controlling DNA repair [40, 41]. PARP is activated by caspases-3 and caspases-7 that facilitate PARP cleavage which is considered a key feature of apoptosis [42, 43]. We examined the effect of NUCKS1 on apoptosis in CRC cells by using these marker proteins. The results confirmed that the levels of p-H$_2$AX and cleaved-PARP were significantly decreased, while Bcl2 levels were increased in NUCKS1-overexpressing CRC cells. Thus, our data suggest that NUCKS1 promotes CRC cell proliferation and inhibits apoptosis.

Similar to apoptosis, autophagy is responsible for maintaining cellular homeostasis [44]. Autophagy plays different roles at different stages of cancer development. In the early stages of tumorigenesis, autophagy serves as a positive pathway to inhibit cancer progression. Once tumors are advanced and subjected to environmental stress, autophagy drives tumor survival and growth [45]. A recent study demonstrated that NUCKS1 could inhibit autophagy through the mTOR-Beclin1 pathway [13]. Next, we evaluated the effect of NUCKS1 on cell autophagy. LC3B plays a key role in autophagy progression and is widely used to assess autophagic activity [46]. Lipidated LC3B recruits P62 to autophagosomes, and P62 is essential for the degradation of protein aggregates and peroxisomes by autophagy [47, 48]. Therefore, we examined the expression levels of LC3B and P62. Lysosomal inhibitors such as CQ and E64d have been used to block autophagy *in vitro*. CQ inhibits autophagy primarily by impairing autophagosome-lysosome fusion [49]. Phosphatidylethanolamine-conjugated LC3B which is known as LC3BII accumulates in cells when CQ or E64d is present to inhibit autophagy [50]. Our study suggests that NUCKS1 knockdown significantly increased autophagy. Cells were fixed, and auto phagolysosomes were detected by transmission electron microscopy imaging. The results
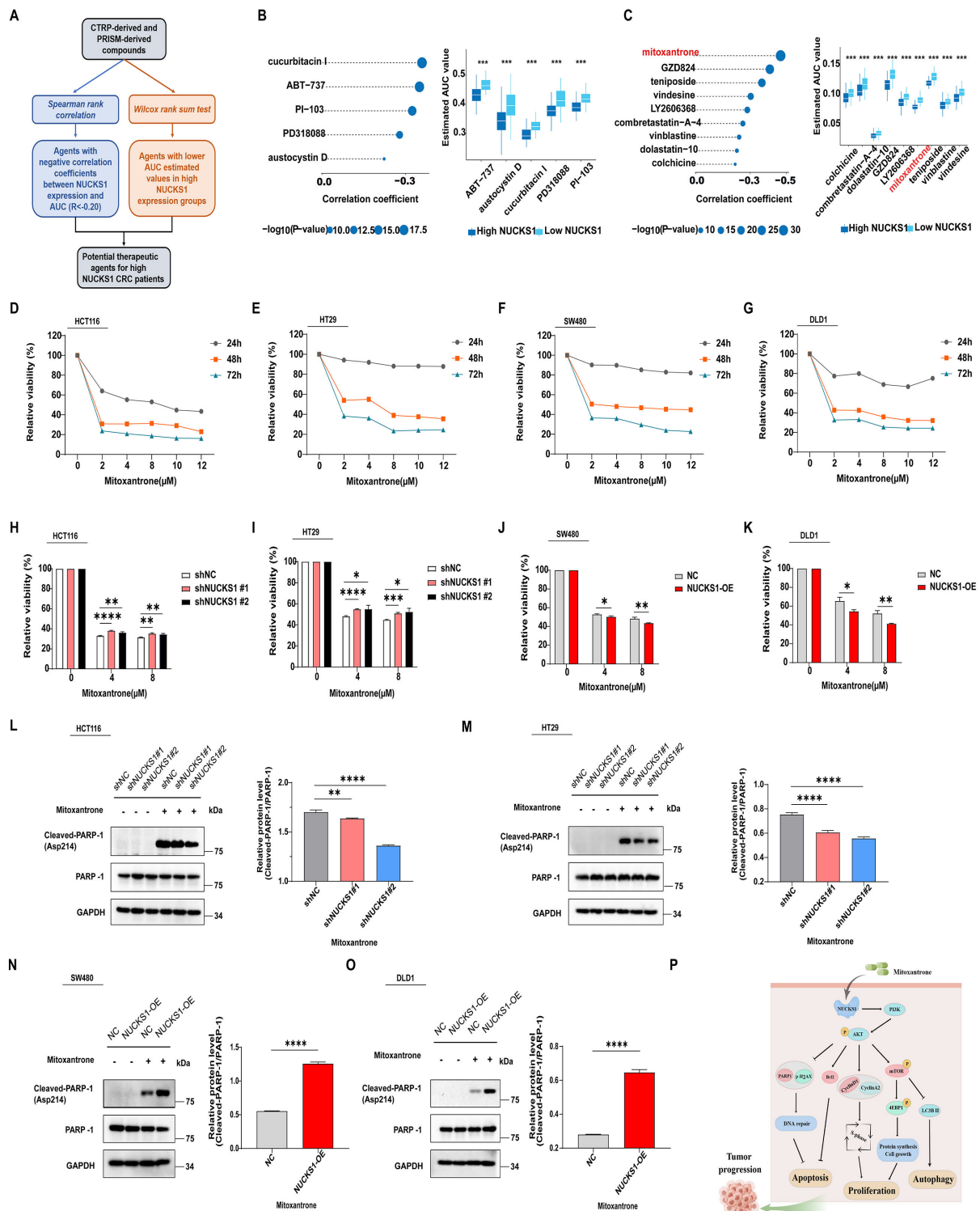
Figure 6. Identification of drugs with greater sensitivity in CRC patients with high NUCKS1 expression. A) Schematic representation of the strategy for identifying candidate drugs. **B)** Analysis of five CTRP-derived compounds. **C)** Analysis of nine PRISM-derived compounds. **D–G)** The cell relative viability in response to different concentrations (2, 4, 8, 10, and 12 μM) of mitoxantrone at 24 h, 48 h, and 72 h according to CCK-8 assay. **H, I)** The cell relative viability of NUCKS1 knockdown cells treated with mitoxantrone was detected by CCK-8 assay. **J, K)** CCK-8 assay was used to assess the cell relative viability of NUCKS1-overexpressing cells treated with mitoxantrone. **L–O)** The levels of cleaved PARP were examined by Western blotting after treatment with mitoxantrone for 48 h. The relative protein level was assessed in NUCKS1 knockdown cells (L–M), and the relative protein level was assessed in NUCKS1-overexpressing cells (N–O). **P)** Schematic diagram of NUCKS1 promoting CRC progression. *p<0.05, **p<0.01, ***p<0.001, ****p<0.0001

indicated that auto phagolysosomes were highly decreased in NUCKS1-overexpressing CRC cells.

Recent studies have elucidated the intersection of autophagy, apoptosis, and cellular homeostasis regulatory circuits [51]. For example, in a variety of important signaling pathways that include PI3K, AKT, and mTOR could suppress apoptosis and inhibit autophagy through signaling stimulation. When the PI3K signaling pathway is downregulated, autophagy or apoptosis may be induced [52]. Previous studies have revealed that the PI3K/AKT/mTOR pathway is involved in regulating cellular events such as promoting tumor growth, progression, motility, and invasion [53–55]. Furthermore, the PI3K/AKT/mTOR pathway is essential in the development as well as in the acquisition of drug resistance of colorectal cancer [30]. mTOR is a key protein in the PI3K/AKT/mTOR pathway that regulates tumor cell growth, proliferation, autophagy, and protein synthesis. The protein 4EBP1 is the best-characterized substrate of mTOR and can regulate protein synthesis that is closely related to cell growth and cell cycle regulation [56]. Therefore, we examined the expression levels of p-AKT, p-mTOR, and p-4EBP1. LY294002 is a specific inhibitor of the PI3K/AKT pathway [57]. In this study, when we used LY294002 to inhibit p-AKT levels in NUCKS1-overexpressing CRC cells, cell proliferation was decreased, and cell apoptosis and autophagy were both increased compared to levels in untreated NUCKS1-overexpressing CRC cells. From these data, we conclude that NUCKS1 promotes CRC progression by activating the PI3K/AKT/mTOR signaling pathway. Next, we will study the downstream molecules regulated by NUCKS1 and their mechanism of action to identify better targets for the treatment of CRC.

Finally, we identified potentially highly sensitive drugs that could target NUCKS1. Five drugs (cucurbitacin I, ABT-737, PI-103, PD318088, austocystin D) were identified via CTRP and nine drugs (mitoxantrone, GZD824, teniposide, vindesine, LY2606368, combretastatin-A-4, vinblastine, dolastatin-10, colchicine) were identified via PRISM. Based on this analysis, we selected mitoxantrone, a chemotherapeutic agent that has been approved for various diseases [58]. Mitoxantrone has exhibited promising clinical efficacy in various malignant tumors, and its clinical response rate is higher when combined with other standard drugs [34]. Thus, we further explored the role of mitoxantrone in NUCKS1 knockdown and overexpression CRC cells. Consistent with this analysis, mitoxantrone exhibited higher drug sensitivity in NUCKS1-overexpressing CRC cells. Moreover, we observed that mitoxantrone can influence CRC cell morphology; however, the exact mechanism remains unclear. Next, we will perform animal experiments using mitoxantrone treatment and elucidate its mechanism of action. Given that the response rate of mitoxantrone monotherapy was lower than that of combination therapy according to previous studies [59], we will further explore the effect of mitoxantrone in combination with chemo-

therapy drugs such as oxaliplatin and 5-fluorouracil or capecitabine for the treatment of CRC.

In summary, our study suggests that NUCKS1 promotes CRC cell proliferation, inhibits apoptosis, and suppresses autophagy by activating the PI3K/AKT/mTOR signaling pathway. For NUCKS1 high-expression CRC patients, mitoxantrone may represent a promising clinical therapeutic agent.

References

[1]   BRAY F, FERLAY J, SOERJOMATARAM I, SIEGEL RL, TORRE LA et al. Global cancer statistics 2018: GLOBOCAN estimates of incidence and mortality worldwide for 36 cancers in 185 countries. CA Cancer J Clin 2018; 68: 394–424. https://doi.org/10.3322/caac.21492

[2]   XIE YH, CHEN YX, FANG JY. Comprehensive review of targeted therapy for colorectal cancer. Signal Transduct Target Ther 2020; 5: 22. https://doi.org/10.1038/s41392-020-0116-z

[3]   LI S, LIU J, ZHENG X, REN L, YANG Y et al. Tumorigenic bacteria in colorectal cancer: Mechanisms and treatments. Cancer Biol Med 2021; 19: 147–162. https://doi.org/10.20892/j.issn.2095-3941.2020.0651

[4]   CHEN W, ZHENG R, ZHANG S, ZENG H, ZUO T et al. Cancer incidence and mortality in China in 2013: An analysis based on urbanization level. Chin J Cancer Res 2017; 29: 1–10. https://doi.org/10.21147/j.issn.1000-9604.2017.01.01

[5]   OSTVOLD AC, HOLTLUND J, LALAND SG. A novel, highly phosphorylated protein, of the high-mobility group type, present in a variety of proliferating and non-proliferating mammalian cells. Eur J Biochem 1985; 153: 469–475. https://doi.org/10.1111/j.1432-1033.1985.tb09325.x

[6]   GRUNDT K, SKJELDAL L, ANTHONSEN HW, SKAUGE T, HUITFELDT HS et al. A putative DNA-binding domain in the NUCKS protein. Arch Biochem Biophys 2002; 407: 168–175. https://doi.org/10.1016/s0003-9861(02)00513-1

[7]   SYMONOWICZ K, DUS-SZACHNIEWICZ K, WOZNIAK M, MURAWSKI M, KOLODZIEJ P et al. Immunohistochemical study of nuclear ubiquitous casein and cyclin-dependent kinase substrate 1 in invasive breast carcinoma of no special type. Exp Ther Med 2014; 8: 1039–1046. https://doi.org/10.3892/etm.2014.1847

[8]   DROSOS Y, KOULOUKOUSSA M, OSTVOLD AC, GRUNDT K, GOUTAS N et al. NUCKS overexpression in breast cancer. Cancer Cell Int 2009; 9: 19. https://doi.org/10.1186/1475-2867-9-19

[9]   CHEONG JY, KIM YB, WOO JH, KIM DK, YEO M et al. Identification of NUCKS1 as a putative oncogene and immunodiagnostic marker of hepatocellular carcinoma. Gene 2016; 584: 47–53. https://doi.org/10.1016/j.gene.2016.03.006

[10] HUME S, GROU CP, LASCAUX P, D'ANGIOLELLA V, LEGRAND AJ et al. The NUCKS1-SKP2-p21/p27 axis controls S phase entry. Nat Commun 2021; 12: 6959. https://doi.org/10.1038/s41467-021-27124-8

[11] GU L, XIA B, ZHONG L, MA Y, LIU L et al. NUCKS1 over-expression is a novel biomarker for recurrence-free survival in cervical squamous cell carcinoma. Tumour Biol 2014; 35: 7831–7836. https://doi.org/10.1007/s13277-014-2035-5

[12] ZHAO S, WANG B, MA Y, KUANG J, LIANG J et al. NU-CKS1 promotes proliferation, invasion and migration of Non-Small cell lung cancer by upregulating CDK1 expression. Cancer Manag Res 2020; 12: 13311–13323. https://doi.org/10.2147/CMAR.S282181

[13] ZHAO E, FENG L, BAI L, CUI H. NUCKS promotes cell proliferation and suppresses autophagy through the mTOR-Beclin1 pathway in gastric cancer. J Exp Clin Cancer Res 2020; 39: 194. https://doi.org/10.1186/s13046-020-01696-7

[14] HUANG YK, KANG WM, MA ZQ, LIU YQ, ZHOU L et al. NUCKS1 promotes gastric cancer cell aggressiveness by upregulating IGF-1R and subsequently activating the PI3K/Akt/mTOR signaling pathway. Carcinogenesis 2019; 40: 370–379. https://doi.org/10.1093/carcin/bgy142

[15] GHANDI M, HUANG FW, JANE-VALBUENA J, KRYU-KOV GV, LO CC et al. Next-generation characterization of the Cancer Cell Line Encyclopedia. Nature 2019; 569: 503–508. https://doi.org/10.1038/s41586-019-1186-3

[16] QIU B, SHI X, WONG ET, LIM J, BEZZI M et al. NUCKS is a positive transcriptional regulator of insulin signaling. Cell Rep 2014; 7: 1876–1886. https://doi.org/10.1016/j.celrep.2014.05.030

[17] INGHAM M, SCHWARTZ GK. Cell-Cycle therapeutics come of age. J Clin Oncol 2017; 35: 2949–2959. https://doi.org/10.1200/JCO.2016.69.0032

[18] ALENZI FQ. Links between apoptosis, proliferation and the cell cycle. Br J Biomed Sci 2004; 61: 99–102. https://doi.org/10.1080/09674845.2004.11732652

[19] HANAHAN D, WEINBERG RA. Hallmarks of cancer: The next generation. Cell 2011; 144: 646–674. https://doi.org/10.1016/j.cell.2011.02.013

[20] DOWNS JA, NUSSENZWEIG MC, NUSSENZWEIG A. Chromatin dynamics and the preservation of genetic information. Nature 2007; 447: 951–958. https://doi.org/10.1038/nature05980

[21] YU L, HOU JG, LI YF, WANG Y, HONG M et al. Inhibiting endoplasmic reticulum stress mediated-autophagy enhances the pro-apoptotic effects of resveratrol derivative in colon cancer cells. Neoplasma 2021; 68: 1236–1244. https://doi.org/10.4149/neo_2021_210422N552

[22] WHITE E. The role for autophagy in cancer. J Clin Invest 2015; 125: 42–46. https://doi.org/10.1172/JCI73941

[23] LEVINE B, KROEMER G. Autophagy in the pathogenesis of disease. Cell 2008; 132: 27–42. https://doi.org/10.1016/j.cell.2007.12.018

[24] LI X, HE S, MA B. Autophagy and autophagy-related proteins in cancer. Mol Cancer 2020; 19: 12. https://doi.org/10.1186/s12943-020-1138-4

[25] PANKIV S, CLAUSEN TH, LAMARK T, BRECH A, BRU-UN JA et al. P62/SQSTM1 binds directly to Atg8/LC3 to facilitate degradation of ubiquitinated protein aggregates by autophagy. J Biol Chem 2007; 282: 24131–2445. https://doi.org/10.1074/jbc.M702824200

[26] SILVA VR, NEVES SP, SANTOS LS, DIAS RB, BEZERRA DP. Challenges and therapeutic opportunities of autophagy in cancer therapy. Cancers (Basel) 2020; 12: 3461. https://doi.org/10.3390/cancers12113461

[27] RAMOS Y, MOBASHERI A. Micrornas and regulation of autophagy in chondrocytes. Methods Mol Biol 2021; 2245: 179–194. https://doi.org/10.1007/978-1-0716-1119-7_13

[28] DUAN S, CHENG J, LI C, YU L, ZHANG X et al. Autophagy inhibitors reduce avian-reovirus-mediated apoptosis in cultured cells and in chicken embryos. Arch Virol 2015; 160: 1679–1685. https://doi.org/10.1007/s00705-015-2415-1

[29] KARAR J, MAITY A. PI3K/AKT/mTOR pathway in angiogenesis. Front Mol Neurosci 2011; 4: 51. https://doi.org/10.3389/fnmol.2011.00051

[30] NARAYANANKUTTY A. PI3K/ akt/ mTOR pathway as a therapeutic target for colorectal cancer: A review of preclinical and clinical evidence. Curr Drug Targets 2019; 20: 1217–1226. https://doi.org/10.2174/1389450120666190618123846

[31] ZHANG T, GUO J, LI H, WANG J. Meta-analysis of the prognostic value of p-4EBP1 in human malignancies. Oncotarget 2018; 9: 2761–2769. https://doi.org/10.18632/oncotarget.23031

[32] HUANG A, ZENG P, LI Y, LU W, LAI Y. LY294002 is a promising inhibitor to overcome sorafenib resistance in FLT3-ITD mutant AML cells by interfering with PI3K/Akt signaling pathway. Front Oncol 2021; 11: 782065. https://doi.org/10.3389/fonc.2021.782065

[33] YANG C, HUANG X, LI Y, CHEN J, LV Y et al. Prognosis and personalized treatment prediction in TP53-mutant hepatocellular carcinoma: An in silico strategy towards precision oncology. Brief Bioinform 2021; 22: bbaa164. https://doi.org/10.1093/bib/bbaa164

[34] KOELLER J, EBLE M. Mitoxantrone: A novel anthracycline derivative. Clin Pharm 1988; 7: 574–581.

[35] EVISON BJ, SLEEBS BE, WATSON KG, PHILLIPS DR, CUTTS SM. Mitoxantrone, more than just another topoisomerase II poison. Med Res Rev 2016; 36: 248–299. https://doi.org/10.1002/med.21364

[36] URREGO D, TOMCZAK AP, ZAHED F, STUHMER W, PARDO LA. Potassium channels in cell cycle and cell proliferation. Philos Trans R Soc Lond B Biol Sci 2014; 369: 20130094. https://doi.org/10.1098/rstb.2013.0094

[37] VERMEULEN K, BERNEMAN ZN, VAN BOCKSTAELE DR. Cell cycle and apoptosis. Cell Prolif 2003; 36: 165–175. https://doi.org/10.1046/j.1365-2184.2003.00267.x

[38] ADAMS JM, CORY S. The Bcl-2 apoptotic switch in cancer development and therapy. Oncogene 2007; 26: 1324–1337. https://doi.org/10.1038/sj.onc.1210220

[39] WILLIS SN, ADAMS JM. Life in the balance: How BH3-only proteins induce apoptosis. Curr Opin Cell Biol 2005; 17: 617–625. https://doi.org/10.1016/j.ceb.2005.10.001

[40] REDON C, PILCH D, ROGAKOU E, SEDELNIKOVA O, NEWROCK K et al. Histone H2A variants H2AX and H2AZ. Curr Opin Genet Dev 2002; 12: 162–169. https://doi.org/10.1016/s0959-437x(02)00282-4

[41]   DICKEY JS, REDON CE, NAKAMURA AJ, BAIRD BJ, SE-DELNIKOVA OA et al. H2AX: Functional roles and potential applications. Chromosoma 2009; 118: 683–692. https://doi.org/10.1007/s00412-009-0234-4

[42]   ISABELLE M, MOREEL X, GAGNE JP, ROULEAU M, ETHIER C et al. Investigation of PARP-1, PARP-2, and PARG interactomes by affinity-purification mass spectrometry. Proteome Sci 2010; 8: 22. https://doi.org/10.1186/1477-5956-8-22

[43]   JUBIN T, KADAM A, JARIWALA M, BHATT S, SUTARIYA S et al. The PARP family: Insights into functional aspects of poly (ADP-ribose) polymerase-1 in cell growth and survival. Cell Prolif 2016; 49: 421–437. https://doi.org/10.1111/cpr.12268

[44]   FUJIWARA Y, FURUTA A, KIKUCHI H, AIZAWA S, HATANAKA Y et al. Discovery of a novel type of autophagy targeting RNA. Autophagy 2013; 9: 403–409. https://doi.org/10.4161/auto.23002

[45]   LI X, HE S, MA B. Autophagy and autophagy-related proteins in cancer. Mol Cancer 2020; 19: 12. https://doi.org/10.1186/s12943-020-1138-4

[46]   SCHAAF MB, KEULERS TG, VOOIJS MA, ROUSCHOP KM. LC3/GABARAP family proteins: Autophagy-(un)related functions. Faseb J 2016; 30: 3961–3978. https://doi.org/10.1096/fj.201600698R

[47]   PANKIV S, CLAUSEN TH, LAMARK T, BRECH A, BRUUN JA et al. P62/SQSTM1 binds directly to Atg8/LC3 to facilitate degradation of ubiquitinated protein aggregates by autophagy. J Biol Chem 2007; 282: 24131–2445. https://doi.org/10.1074/jbc.M702824200

[48]   SHVETS E, ABADA A, WEIDBERG H, ELAZAR Z. Dissecting the involvement of LC3B and GATE-16 in p62 recruitment into autophagosomes. Autophagy 2011; 7: 683–688. https://doi.org/10.4161/auto.7.7.15279

[49]   MAUTHE M, ORHON I, ROCCHI C, ZHOU X, LUHR M et al. Chloroquine inhibits autophagic flux by decreasing autophagosome-lysosome fusion. Autophagy 2018; 14: 1435–1455. https://doi.org/10.1080/15548627.2018.1474314

[50]   OH SY, HWANG JR, CHOI M, KIM YM, KIM JS et al. Autophagy regulates trophoblast invasion by targeting NF-kappaB activity. Sci Rep 2020; 10: 14033. https://doi.org/10.1038/s41598-020-70959-2

[51]   LEVINE B, KROEMER G. Autophagy in the pathogenesis of disease. Cell 2008; 132: 27–42. https://doi.org/10.1016/j.cell.2007.12.018

[52]   MATHEW R, KARANTZA-WADSWORTH V, WHITE E. Role of autophagy in cancer. Nat Rev Cancer 2007; 7: 961–967. https://doi.org/10.1038/nrc2254

[53]   STEFANI C, MIRICESCU D, STANESCU-SPINU II, NICA RI, GREABU M et al. Growth factors, PI3K/AKT/mTOR and MAPK signaling pathways in colorectal cancer pathogenesis: Where are we now? Int J Mol Sci 2021; 22: 10260. https://doi.org/10.3390/ijms221910260

[54]   DUAN S, HUANG W, LIU X, LIU X, CHEN N et al. IMPDH2 promotes colorectal cancer progression through activation of the PI3K/AKT/mTOR and PI3K/AKT/FOXO1 signaling pathways. J Exp Clin Cancer Res 2018; 37: 304. https://doi.org/10.1186/s13046-018-0980-3

[55]   MA Z, LOU S, JIANG Z. PHLDA2 regulates EMT and autophagy in colorectal cancer via the PI3K/AKT signaling pathway. Aging (Albany NY) 2020; 12: 7985–8000. https://doi.org/10.18632/aging.103117

[56]   WANG Y, ZHANG H. Regulation of autophagy by mTOR signaling pathway. Adv Exp Med Biol 2019; 1206: 67–83. https://doi.org/10.1007/978-981-15-0602-4_3

[57]   ZAJĄC A, SUMOREK-WIADRO J, MACIEJCZYK A, LANGNER E, WERTEL I et al. LY294002 and sorafenib as inhibitors of intracellular survival pathways in the elimination of human glioma cells by programmed cell death. Cell Tissue Res 2021; 386: 17–28. https://doi.org/10.1007/s00441-021-03481-0

[58]   CHANG A. A case of mitoxantrone extravasation. J Oncol Pharm Pract 2020; 26: 1270–1273. https://doi.org/10.1177/1078155219893736

[59]   BURGESS KE, DEREGIS CJ. Urologic oncology. Vet Clin North Am Small Anim Pract 2019; 49: 311–323. https://doi.org/10.1016/j.cvsm.2018.11.006